

Atomic data from the IRON Project

XXII. Radiative rates for forbidden transitions within the ground configuration of ions in the carbon and oxygen isoelectronic sequences*

M.E. Galavís^{1,3}, C. Mendoza², and C.J. Zeippen³

¹ Departamento de Física, Universidad Metropolitana, PO Box 76819, Caracas 1070A, Venezuela

² Centro de Física, Instituto Venezolano de Investigaciones Científicas (IVIC), PO Box 21827, Caracas 1020A, Venezuela

³ URA 173 (associée au CNRS et à l'Université Paris 7) et DAEC, Observatoire de Paris, F-92195 Meudon, France

Received September 16; accepted September 17, 1996

Abstract. As part of the IRON Project, radiative rates have been calculated for the forbidden transitions within the ground configuration of atoms and ions in the carbon ($2s^22p^2$) and oxygen ($2s^22p^4$) isoelectronic sequences for $Z \leq 28$. The atomic structure code SUPERSTRUCTURE was used, which allows for configuration interaction, relativistic effects and semi-empirical term energy corrections. Comparisons are made with previous theoretical datasets for the same sequences. It is shown once again that, to obtain reliable transition probabilities, in particular those of the electric quadrupole type, it is essential to use accurate and consistent experimental transition wavelengths. For the C and O sequences such data are fortunately available from the work of Edlén (1983, 1985). The general accuracy of the present probabilities is rated to be within 10%, with the exception of some electric quadrupole transitions in low- Z ions whose radiative rates are small with an accuracy not better than $\pm 50\%$.

Key words: atomic data — atomic processes

1. Introduction

The IRON Project (IP, see the general description by Hummer et al. 1993) is an international collaboration primarily concerned with the computation of reliable electron excitation rates for ions of astrophysical interest, with an emphasis on the heavier species belonging to the iron group. The IP has been motivated by data requirements from recent ambitious satellite-borne telescope missions such as the Infrared Space Observatory (ISO), the

Send offprint requests to: C.J. Zeippen

* A detailed table of the present E2 and M1 transition probabilities is available in electronic form from the CDS via anonymous ftp 130.79.128.5

Space Infrared Telescope Facility (SIRTF) and the Solar and Heliospheric Observatory (SOHO). Another aim of the IP is to produce quality radiative data such as oscillator strengths, transition probabilities and photoionisation cross sections to help satisfy users' needs. Indeed, the practical value of the future IP public databases will be greatly enhanced if, for example, accurate collisional and radiative rates are included for the same transitions. The policy of the IP is to calculate new data rather than to compile results from existing work. In fact, it is frequently difficult to assign accuracy ratings to older theoretical datasets. Also, the evolution of computers and the development of computational methods are an encouragement to revisit important cases. In the present report, the forbidden transitions within the ground configuration of the carbon ($2s^22p^2$) and oxygen ($2s^22p^4$) isoelectronic sequences are considered. It should be noted that there is no previous full-scale study of the oxygen sequence by means of the code SUPERSTRUCTURE.

The forbidden transitions in C-like ions were previously considered by Garstang (1968), Nicolaides et al. (1971), Nussbaumer (1971), Kastner et al. (1977), Mason & Bhatia (1978), Nussbaumer & Rusca (NR, 1979), Cheng et al. (1979), Baluja & Doyle (1981), and more recently by Froese Fischer & Saha (FS1, 1985) and Hibbert et al. (1993). For ions in the oxygen sequence, computations have been reported by Garstang (1968), Nicolaides et al. (1971), Kastner et al. (1977), Cheng et al. (1979), Bhatia et al. (1979), Froese Fischer & Saha (FS2, 1983), Baluja & Zeippen (BZ, 1988) and Gaigalas et al. (1994). Note that the references given above are the most directly relevant to the present work. For a more complete bibliography see Biémont & Zeippen (1991, 1996). Since we are concerned here with radiative datasets for complete sequences rather than for specific systems, we will focus our comparisons on the extensive datasets generated by

NR, FS1, BZ and FS2. It is worth noting that the general agreement among these datasets is found to be unsatisfactory: only 76% of the A -values in NR and FS1 (C sequence) and 71% in BZ and FS2 (O sequence) agree to within 10%. The worse differences are as large as an order of magnitude. It is important to try and shed some light on the reasons for such discrepancies. The extensive study by Cheng et al. (1979) will not be compared in detail with the present work because these authors restrict correlation in their physical models to the $n = 2$ complex. They were mainly concerned with treating relativistic effects “fully” in a Dirac-Fock formalism. As discussed in BZ, their resulting transition probabilities are accurate for higher atomic numbers, but lack reliability for the lighter elements at the neutral end of a given isoelectronic sequence.

The present attempt aims at generating datasets of high reliability (i.e. with accuracy ratings of 10% or better) to be incorporated in the IP databases. We make use of the computer program SUPERSTRUCTURE (Eissner et al. 1974; Nussbaumer & Storey 1978; Eissner 1991), which allows for configuration interaction (CI) and Breit-Pauli (BP) relativistic effects. This code has been extensively applied in the computation of atomic spectra. The numerical method is described in Sect. 2, followed by an analysis of the present results in Sect. 3. Concluding remarks are given in Sect. 4.

2. Method

The computer program SUPERSTRUCTURE was originally developed by Eissner et al. (1974), and the version used in the present work contains improvements by Nussbaumer & Storey (1978). A summary of the code’s main features is given by Eissner (1991). In this approach the wavefunctions are expressed in a configuration expansion of the type

$$\Psi = \sum_i \phi_i c_i , \quad (1)$$

where the basis functions ϕ_i are constructed from one-electron orbitals generated in two types of potential $V(\lambda_{nl})$: spectroscopic orbitals $P(nl)$ are calculated in a statistical Thomas–Fermi–Dirac model potential (Eissner & Nussbaumer 1969) whereas correlation orbitals $P(\bar{n}l)$ are obtained in a Coulomb potential (Nussbaumer & Storey 1978). The scaling parameters λ_{nl} are computed variationally so as to minimize the weighted sum of the non-relativistic energies of the terms of the ground configuration

$$\mathcal{F} = g_1 E(^3P) + g_2 E(^1D) + g_3 E(^1S) , \quad (2)$$

where g_i denotes the usual statistical weight. The selection of the configuration basis set for each sequence requires some attention. Of course, the aim is to get level energies as close as possible to experimental values, but it is

also of primary importance to build a well-balanced physical model. Indeed, an excessively intricate description of a given atomic system may introduce spurious numerical effects which can affect considerably the calculated transition rates even when the level energies turn out to be accurate. The configuration representations and scaling parameters used in this work are listed in Tables 1–3.

Table 1. Configuration basis sets selected for the present calculations. Term symmetries 3P , 1D and 1S are the only ones retained in the physical model

C Sequence	O Sequence
$2s^2 2p^2$	$2s^2 2p^4$
$2p^4$	$2p^6$
$2s^2 2p\bar{3}p$	$2s^2 2p^3\bar{3}p$
$2s^2\bar{3}s\bar{3}d$	$2s2p^4\bar{3}s$
$2s2p^2\bar{3}s$	$2s2p^4\bar{3}d$
$2s2p^2\bar{3}d$	$2s^2 2p^2\bar{3}p^2$
$2p^3\bar{3}p$	$2s^2 2p^2\bar{3}d^2$
$2s^2\bar{3}s^2$	$2s2p^3\bar{3}s\bar{3}p$
$2s^2\bar{3}p^2$	$2s^2 2p^3\bar{4}p$
$2s^2\bar{3}d^2$	$2s^2 2p^3\bar{4}f$
$2s2p\bar{3}s\bar{3}p$	$2s^2 2p^2\bar{3}p\bar{4}p$
$2s2p\bar{3}p\bar{3}d$	$2s^2 2p^2\bar{3}s^2$
$2p^2\bar{3}s\bar{3}d$	
$2p^2\bar{3}s^2$	
$2p^2\bar{3}p^2$	
$2p^2\bar{3}d^2$	
$2s^2 2p\bar{4}f$	
$2s2p\bar{3}d\bar{4}f$	

In SUPERSTRUCTURE the Hamiltonian is taken to be of the form

$$H = H_{\text{nr}} + H_{\text{bp}} \quad (3)$$

where H_{nr} is the usual non-relativistic Hamiltonian and H_{bp} is the BP relativistic correction (Jones 1970, 1971; Eissner et al. 1974; Eissner 1991). Using perturbation theory, the relativistic wavefunction ψ_i^{r} can be expanded in terms of the non-relativistic functions ψ_j^{nr} :

$$\psi_i^{\text{r}} = \psi_i^{\text{nr}} + \sum_{j \neq i} \psi_j^{\text{nr}} \times \frac{\langle \psi_j^{\text{nr}} | H_{\text{bp}} | \psi_i^{\text{nr}} \rangle}{E_i^{\text{nr}} - E_j^{\text{nr}}} + \dots \quad (4)$$

Small fractional errors in the non-relativistic energies E_i^{nr} and E_j^{nr} can lead to much larger errors in the differences $E_i^{\text{nr}} - E_j^{\text{nr}}$ for $j \neq i$. Using experimental data, improved estimates of the non-relativistic energies can be obtained and a modified H_{nr} can be constructed. This semi-empirical term energy correction (TEC) procedure was implemented in SUPERSTRUCTURE by Zeippen et al. (1977). In the present case, the corrections are chosen so as to move the computed energies of the

Table 2. Scaling parameters used to generate the orbitals for the C-like ions. The negative scaling parameters denote correlation Coulombic orbitals

Ion	λ_{1s}	λ_{2s}	λ_{2p}	$\lambda_{\bar{3}s}$	$\lambda_{\bar{3}p}$	$\lambda_{\bar{3}d}$	$\lambda_{\bar{4}f}$
C I	1.488	1.216	1.174	-0.875	-0.654	-0.956	-1.553
N II	1.484	1.221	1.327	-0.985	-0.959	-1.058	-1.765
O III	1.481	1.278	1.364	-1.067	-1.065	-1.139	-1.918
F IV	1.479	1.327	1.387	-1.126	-1.137	-1.200	-2.033
Ne V	1.477	1.427	0.972	-1.147	-0.933	-1.256	-2.123
Na VI	1.477	1.102	0.932	-1.092	-0.983	-1.293	-2.188
Mg VII	1.475	1.068	0.886	-1.118	-1.027	-1.324	-2.247
Al VIII	1.474	1.050	0.839	-1.141	-1.066	-1.351	-2.295
Si IX	1.473	1.047	0.793	-1.161	-1.101	-1.373	-2.336
P X	1.472	1.053	0.748	-1.176	-1.132	-1.392	-2.372
S XI	1.471	1.059	0.704	-1.189	-1.160	-1.409	-2.402
Cl XII	1.470	1.069	0.669	-1.201	-1.185	-1.424	-2.429
Ar XIII	1.469	1.077	0.635	-1.211	-1.208	-1.437	-2.453
K XIV	1.469	1.086	0.606	-1.220	-1.229	-1.449	-2.475
Ca XV	1.466	1.093	0.582	-1.228	-1.247	-1.459	-2.494
Sc XVI	1.468	1.099	0.559	-1.235	-1.264	-1.469	-2.511
Ti XVII	1.467	1.105	0.538	-1.242	-1.280	-1.477	-2.527
V XVIII	1.467	1.110	0.523	-1.248	-1.294	-1.485	-2.541
Cr XIX	1.466	1.112	0.508	-1.254	-1.307	-1.492	-2.555
Mn XX	1.466	1.120	0.495	-1.259	-1.319	-1.499	-2.567
Fe XXI	1.466	1.122	0.488	-1.264	-1.329	-1.505	-2.578
Co XXII	1.466	1.125	0.473	-1.270	-1.340	-1.511	-2.588
Ni XXIII	1.465	1.130	0.471	-1.273	-1.348	-1.516	-2.597

Table 3. Scaling parameters used to generate the orbitals for the O-like ions. The negative scaling parameters denote correlation Coulombic orbitals

Ion	λ_{1s}	λ_{2s}	λ_{2p}	λ_{3s}	λ_{3p}	λ_{3d}	λ_{4p}	λ_{4f}
O I	1.497	1.039	1.096	-1.011	-0.836	-1.000	-0.886	-1.0
F II	1.486	1.089	1.100	-1.036	-0.917	-1.091	-1.031	-1.0
Ne III	1.478	1.319	1.090	-0.999	-0.961	-1.162	-1.194	-1.0
Na IV	1.468	1.320	1.093	-1.036	-1.015	-1.218	-1.272	-1.0
Mg V	1.462	1.276	1.098	-1.068	-1.064	-1.262	-1.329	-1.0
Al VI	1.456	1.220	1.093	-1.100	-1.102	-1.302	-1.364	-1.0
Si VII	1.440	1.183	1.084	-1.136	-1.131	-1.340	-1.400	-1.0
P VIII	1.434	1.166	1.073	-1.161	-1.148	-1.367	-1.427	-1.0
S IX	1.431	1.157	1.064	-1.180	-1.161	-1.392	-1.454	-1.0
Cl X	1.428	1.158	1.059	-1.190	-1.174	-1.410	-1.484	-1.0
Ar XI	1.426	1.151	1.059	-1.202	-1.192	-1.438	-1.510	-1.0
K XII	1.424	1.150	1.059	-1.210	-1.210	-1.454	-1.539	-1.0
Ca XIII	1.422	1.150	1.060	-1.220	-1.218	-1.468	-1.558	-1.0
Sc XIV	1.420	1.150	1.061	-1.228	-1.232	-1.482	-1.580	-1.0
Ti XV	1.418	1.150	1.062	-1.236	-1.245	-1.494	-1.602	-1.0
V XVI	1.417	1.150	1.064	-1.243	-1.257	-1.506	-1.610	-1.0
Cr XVII	1.414	1.151	1.065	-1.249	-1.269	-1.510	-1.632	-1.0
Mn XVIII	1.414	1.151	1.067	-1.256	-1.280	-1.532	-1.647	-1.0
Fe XIX	1.413	1.152	1.070	-1.261	-1.294	-1.540	-1.662	-1.0
Co XX	1.412	1.152	1.069	-1.267	-1.301	-1.548	-1.674	-1.0
Ni XXI	1.411	1.153	1.071	-1.272	-1.310	-1.555	-1.686	-1.0

terms ^1D and ^1S in each ion to match the observed term separation. Previous work has shown that the TEC procedure is efficient and reliable when the corrections are small, i.e. when the ab initio wavefunctions represent the system under consideration with very good accuracy.

The total radiative rate for a forbidden transition is taken to be the sum of the electric quadrupole (E2) and magnetic dipole (M1) contributions

$$A_{ij} = A_{ij}(\text{E2}) + A_{ij}(\text{M1}), \quad (5)$$

with

$$A_{ij}(\text{E2}) = 2.6733 \cdot 10^3 (E_i - E_j)^5 \frac{1}{g_i} S_{ij}^{E2} \quad (\text{s}^{-1}) \quad (6)$$

and

$$A_{ij}(\text{M1}) = 3.5644 \cdot 10^4 (E_i - E_j)^3 \frac{1}{g_i} S_{ij}^{M1} \quad (\text{s}^{-1}). \quad (7)$$

Here g_i is the statistical weight of the level i and energies E are expressed in Rydbergs. From Eqs. (6) and (7), it is clear that the accuracy of the calculated A -values depends strongly on the quality of the wavefunctions used for evaluating the line strengths S . Moreover one can see that a relatively small error in the energy difference ($E_i - E_j$) can mar an otherwise reliable calculation: note the exponents 5 and 3 respectively in Eqs. (6) and (7). To eliminate such a drastic cause of inaccuracy, experimental level separations from the extensive work of Edlén (1983, 1985) have replaced computed energies in this work.

3. Results

3.1. The carbon isoelectronic sequence

Since we are using the same numerical method as NR, we have attempted to refine their calculation by increasing the configuration expansion. It is found that some excitation energies can be considerably improved by this procedure, particularly for species with $Z \leq 11$. The two configurations involving $P(4f)$ orbitals which are listed in Table 1 contribute towards a very accurate ^1D level energy for all ions in the sequence. This contrasts with the relatively large discrepancies found for low Z by NR with respect to experiment. The ^1S level remains virtually unaffected by the inclusion of $P(4f)$ orbitals in the physical model. The inclusion of other $P(4l)$ orbitals was found to be unimportant in all cases. We finally settled for the 18-configuration representation listed in Table 1, which appears to be more “realistic” than the 11-configuration set of NR: it contains all even configurations with one or two excitations in $n = 3$ and a closed $1s^2$ plus the important $2s^22p4f$ and $2s2p3d4f$ configurations. The resulting level excitation energies are given in Table 4 together with the experimental, NR and FS1 data. The FS1 data were computed with the Multiconfiguration Hartree-Fock method plus Breit-Pauli relativistic corrections (MCHF +

BP) and an extensive configuration expansion including states with $n \leq 4$. Throughout the sequence, the present ^1D separations agree better with experiment than the FS1 results. For all other energies the agreement between the FS1 data, the present findings and experiment is within 5%.

The present total transition probabilities are listed in Table 5, together with the NR and FS1 datasets. Note that for most spectral lines either the M1 or the E2 type transition dominates. The level of agreement with NR is good: 86% of the data agree to within 10% (see Fig. 1a). Large differences (up to 63%) are mostly found for the $^3\text{P}_0 - ^1\text{D}_2$ E2 transition, in particular for $Z = 6 - 9$ and $Z = 25$. These transitions have relatively small line strengths and are sensitive to the level separation in Eq. (6) and to the TECs. For low Z , the A -value is also sensitive to CI and to the spin–spin relativistic interaction. The differences for $Z = 6 - 9$ are therefore explicable in terms of the present improved CI expansion and perhaps of a more extensive treatment of the spin–spin contributions, while that for $Z = 25$ is due to an anomalously high NR A -value. Note that this sensitive transition probability does not differ very much in the present work whether or not the two configurations containing $P(4f)$ orbitals are taken into account. This illustrates that a small deficit in CI can be compensated by a slightly larger TEC value. Thus, the validity of the TEC procedure is confirmed.

The comparison with the FS1 work (see Fig. 1b) is less impressive as only 72% of the data agree to 10%, with big discrepancies (as large as a factor of 9) for the sensitive $^3\text{P}_0 - ^1\text{D}_2$ transitions in both lowly and highly ionised systems. Since FS1 evaluated their A -values with computed energies, which can result in large errors (see end of Sect. 2), their results were corrected using the experimental transition wavelengths (see FS1c in Table 5 and Fig. 1c). Although the large differences for the $^3\text{P}_0 - ^1\text{D}_2$ transitions are significantly reduced, the number of cases lying within the required $\pm 10\%$ range is not increased. It is found that, while the accord for some A -values is improved by this procedure, for others it is actually made worse cancelling out the positive changes.

At this stage it is worth considering Garstang’s (1968) classic study who computed radiative transition probabilities for forbidden lines at the lower end of the carbon and oxygen sequences. His Hamiltonian included terms arising from the spin-orbit, mutual spin-orbit and spin–spin interactions, and his Hartree-Fock (HF) wavefunctions were adjusted to fit experimental energies. There is good agreement between his work and ours for the problematic $^3\text{P}_0 - ^1\text{D}_2$ transition indicating a high sensitivity to relativistic effects with emphasis on the spin–spin interaction.

There is an extensive study of astrophysically important transitions in neutral carbon by Hibbert et al. (1993) who used the code CIV3. They treated mainly electric dipole (E1) transitions but they

Table 4. Experimental and calculated excitation energies in cm^{-1} from the $2s^22p^2\ ^3P_0$ ground state for the carbon sequence. Expt: experiment Edlén (1983, 1985). Pres: present results. NR: Nussbaumer & Rusca (1979). FS1: Froese Fischer & Saha (1985)

Z	State	Expt	Pres	NR	FS1	Z	State	Expt	Pres	NR	FS1
6	3P_1	16.4	16.5	17	16	18	3P_1	9859	9901		9878
	3P_2	43.4	44.2	44	42		3P_2	21850	22124		21964
	1D_2	10192.6	10516.6	11911	10989		1D_2	85026	86572		87680
	1S_0	21648.0	22305.5	23196	22204		1S_0	162158	164509		162832
7	3P_1	48.7	49.1		48	19	3P_1	13248	13337		13285
	3P_2	130.8	128.7		128		3P_2	28235	28628		28433
	1D_2	15316.3	16009.4		16307		1D_2	95944	97629		99142
	1S_0	32688.9	34524.6		33285		1S_0	178961	181362		179751
8	3P_1	114	113	113	112	20	3P_1	17555	17713	17638	17628
	3P_2	307	300	303	302		3P_2	35917	36464	36183	36261
	1D_2	20274	21041	21988	21389		1D_2	108595	110451	110949	112517
	1S_0	43186	45223	44937	43809		1S_0	197648	200122	199507	198559
9	3P_1	226	226		225	21	3P_1	22959	23222		23058
	3P_2	615	602		609		3P_2	45030	45794		45567
	1D_2	25236	26043		26429		1D_2	123349	125419		128167
	1S_0	53538	55662		54159		1S_0	218583	221159		219774
10	3P_1	413	403		409	22	3P_1	29660	30069		29809
	3P_2	1111	1107		1104		3P_2	55728	56768		56577
	1D_2	30291	31152		31540		1D_2	140626	142961		146585
	1S_0	63915	65771		64513		1S_0	242169	244893		243676
11	3P_1	698	685		692	23	3P_1	37869	38485		38085
	3P_2	1858	1861		1851		3P_2	68155	69552		69462
	1D_2	35506	36540		36809		1D_2	160882	163554		168248
	1S_0	74423	76549		74993		1S_0	268834	271769		270760
12	3P_1	1118	1101	1104	1110	24	3P_1	47811	48708		48118
	3P_2	2933	2942	2907	2925		3P_2	82461	84307		84428
	1D_2	40957	42039	42756	42322		1D_2	184608	187702		193682
	1S_0	85163	87340	87127	85707		1S_0	299032	302265		301506
13	3P_1	1715	1696		1707	25	3P_1	59723	61003		60148
	3P_2	4419	4442		4413		3P_2	98804	101224		101701
	1D_2	46729	47861		48176		1D_2	212320	215952		223438
	1S_0	96243	98453		96770		1S_0	333240	336887		336416
14	3P_1	2546	2528		2539	26	3P_1	73852	75637	75254	74426
	3P_2	6415	6460		6416		3P_2	117362	120497	119850	121533
	1D_2	52927	54115		54489		1D_2	244546	248851	249749	258086
	1S_0	107792	110026		108312		1S_0	371954	376162	375964	376018
15	3P_1	3682	3668		3679	27	3P_1	90450	92886		91211
	3P_2	9031	9109		9044		3P_2	138330	142355		144204
	1D_2	59681	60935		61397		1D_2	281817	286959		298214
	1S_0	119960	122214		120393		1S_0	415681	420632		420854
16	3P_1	5208	5203		5208	28	3P_1	109780	113046		110770
	3P_2	12388	12511		12418		3P_2	161928	167041		170026
	1D_2	67147	68484		69089		1D_2	324674	330857		344424
	1S_0	132929	135211		133478		1S_0	464950	470866		471489
17	3P_1	7227	7238		7234						
	3P_2	16616	16801		16677						
	1D_2	75520	76950		77763						
	1S_0	146912	149224		147508						

also give results for the forbidden transitions in the ground configuration. Concerning the large $^1D_2 - ^1S_0$ E2 transition probability, there is excellent agreement between the CIV3, FS1c and present A -value. This confirms the carbon abundance in the sun proposed by Biémont et al. (1993). The NR result for this transition appears to be underestimated by some 20%, just as the probability reported by Nicolaides et al. (1971) who used the “charge-distribution” (CD) concept.

In conclusion the discrepancies between the FS1 data and the SUPERSTRUCTURE results (NR and present), appear to be due to real differences in the line strengths. This is most probably linked to the use of the TEC procedure in the latter calculations. Further conclusions will be drawn after the analysis of the data for the oxygen sequence.

Table 5. Transition probabilities in s^{-1} within the ground state configuration of the carbon sequence. Pres: present results. NR: Nussbaumer & Rusca (1979). FS1: Froese Fischer & Saha (1985). FS1c: FS1 corrected with the experimental wavelengths. $a \pm b$ denotes $a \times 10^{\pm b}$

Z	Trans	Pres	NR	FS1	FS1c	Z	Trans	Pres	NR	FS1	FS1c
6	$^3\text{P}_0-^3\text{P}_1$	7.932–8	7.93–8	7.303–8	7.865–8	12	$^3\text{P}_0-^3\text{P}_1$	2.510–2	2.57–2	2.456–2	2.509–2
	$^3\text{P}_0-^3\text{P}_2$	2.054–14	1.71–14	1.613–14	1.900–14		$^3\text{P}_0-^3\text{P}_2$	2.319–7	2.40–7	2.369–7	2.402–7
	$^3\text{P}_1-^3\text{P}_2$	2.654–7	2.65–7	2.336–7	2.616–7		$^3\text{P}_1-^3\text{P}_2$	8.052–2	8.02–2	8.051–2	8.051–2
	$^3\text{P}_0-^1\text{D}_2$	5.923–8	7.77–8	1.157–7	7.943–8		$^3\text{P}_0-^1\text{D}_2$	1.163–4	1.37–4	1.711–4	1.452–4
	$^3\text{P}_1-^1\text{D}_2$	7.467–5	8.21–5	7.465–5	5.992–5		$^3\text{P}_1-^1\text{D}_2$	1.192+0	1.22+0	1.269+0	1.147+0
	$^3\text{P}_2-^1\text{D}_2$	2.229–4	2.44–4	2.231–4	1.776–4		$^3\text{P}_2-^1\text{D}_2$	3.107+0	3.18+0	3.324+0	2.989+0
	$^3\text{P}_1-^1\text{S}_0$	2.382–3	2.71–3	2.248–3	2.083–3		$^3\text{P}_1-^1\text{S}_0$	3.585+1	3.70+1	3.687+1	3.615+1
	$^3\text{P}_2-^1\text{S}_0$	2.117–5	2.00–5	1.822–5	1.604–5		$^3\text{P}_2-^1\text{S}_0$	3.611–2	3.81–2	3.700–2	3.578–2
	$^1\text{D}_2-^1\text{S}_0$	6.424–1	5.28–1	5.666–1	6.300–1		$^1\text{D}_2-^1\text{S}_0$	3.958+0	4.04+0	3.746+0	4.114+0
	$^3\text{P}_0-^3\text{P}_1$	2.077–6	2.08–6	1.966–6	2.053–6	13	$^3\text{P}_0-^3\text{P}_1$	9.052–2	9.07–2	8.921–2	9.047–2
7	$^3\text{P}_0-^3\text{P}_2$	1.127–12	1.16–12	1.062–12	1.183–12		$^3\text{P}_0-^3\text{P}_2$	1.185–6	1.22–6	1.219–6	1.227–6
	$^3\text{P}_1-^3\text{P}_2$	7.463–6	7.46–6	6.830–6	7.382–6		$^3\text{P}_1-^3\text{P}_2$	2.660–1	2.66–1	2.668–1	2.662–1
	$^3\text{P}_0-^1\text{D}_2$	3.554–7	5.35–7	7.586–7	5.545–7		$^3\text{P}_0-^1\text{D}_2$	2.495–4	2.92–4	3.597–4	3.088–4
	$^3\text{P}_1-^1\text{D}_2$	1.016–3	1.01–3	1.001–3	8.288–4		$^3\text{P}_1-^1\text{D}_2$	3.116+0	3.19+0	3.298+0	2.998+0
	$^3\text{P}_2-^1\text{D}_2$	3.005–3	2.99–3	2.966–3	2.452–3		$^3\text{P}_2-^1\text{D}_2$	7.746+0	7.93+0	8.246+0	7.451+0
	$^3\text{P}_1-^1\text{S}_0$	3.297–2	3.38–2	3.086–2	2.923–2		$^3\text{P}_1-^1\text{S}_0$	8.983+1	9.22+1	9.204+1	9.049+1
	$^3\text{P}_2-^1\text{S}_0$	1.315–4	1.51–4	1.409–4	1.286–4		$^3\text{P}_2-^1\text{S}_0$	7.605–2	8.00–2	7.743–2	7.522–2
	$^1\text{D}_2-^1\text{S}_0$	1.023+0	1.12+0	1.085+0	1.217+0		$^1\text{D}_2-^1\text{S}_0$	4.544+0	4.62+0	4.298+0	4.721+0
	$^3\text{P}_0-^3\text{P}_1$	2.664–5	2.64–5	2.523–5	2.591–5	14	$^3\text{P}_0-^3\text{P}_1$	2.958–1	3.11–1	2.934–1	2.958–1
	$^3\text{P}_0-^3\text{P}_2$	3.094–11	3.19–11	3.027–11	3.233–11		$^3\text{P}_0-^3\text{P}_2$	5.242–6	5.56–6	5.429–6	5.425–6
8	$^3\text{P}_1-^3\text{P}_2$	9.695–5	9.70–5	9.248–5	9.693–5		$^3\text{P}_1-^3\text{P}_2$	7.777–1	7.78–1	7.823–1	7.775–1
	$^3\text{P}_0-^1\text{D}_2$	1.690–6	2.39–6	3.276–6	2.507–6		$^3\text{P}_0-^1\text{D}_2$	5.027–4	5.81–4	7.162–4	6.193–4
	$^3\text{P}_1-^1\text{D}_2$	6.995–3	6.97–3	7.148–3	6.081–3		$^3\text{P}_1-^1\text{D}_2$	7.535+0	7.66+0	7.931+0	7.234+0
	$^3\text{P}_2-^1\text{D}_2$	2.041–2	2.03–2	2.091–2	1.775–2		$^3\text{P}_2-^1\text{D}_2$	1.772+1	1.80+1	1.878+1	1.701+1
	$^3\text{P}_1-^1\text{S}_0$	2.268–1	2.32–1	2.218–1	2.124–1		$^3\text{P}_1-^1\text{S}_0$	2.064+2	2.11+2	2.108+2	2.077+2
	$^3\text{P}_2-^1\text{S}_0$	6.091–4	6.83–4	6.556–4	6.097–4		$^3\text{P}_2-^1\text{S}_0$	1.509–1	1.59–1	1.524–1	1.486–1
	$^1\text{D}_2-^1\text{S}_0$	1.561+0	1.70+0	1.608+0	1.792+0		$^1\text{D}_2-^1\text{S}_0$	5.154+0	5.31+0	4.861+0	5.350+0
	$^3\text{P}_0-^3\text{P}_1$	2.075–4	2.05–4	2.053–4	2.080–4	15	$^3\text{P}_0-^3\text{P}_1$	8.929–1	8.97–1	8.903–1	8.925–1
	$^3\text{P}_0-^3\text{P}_2$	4.727–10	4.79–10	4.764–10	5.003–10		$^3\text{P}_0-^3\text{P}_2$	2.061–5	2.15–5	2.149–5	2.134–5
9	$^3\text{P}_1-^3\text{P}_2$	7.937–4	7.82–4	7.643–4	7.945–4		$^3\text{P}_1-^3\text{P}_2$	2.049+0	2.08+0	2.069+0	2.051+0
	$^3\text{P}_0-^1\text{D}_2$	6.124–6	8.24–6	1.093–5	8.676–6		$^3\text{P}_0-^1\text{D}_2$	9.627–4	1.10–3	1.370–3	1.189–3
	$^3\text{P}_1-^1\text{D}_2$	3.398–2	3.39–2	3.523–2	3.063–2		$^3\text{P}_1-^1\text{D}_2$	1.712+1	1.74+1	1.794+1	1.639+1
	$^3\text{P}_2-^1\text{D}_2$	9.731–2	9.72–2	1.012–1	8.770–2		$^3\text{P}_2-^1\text{D}_2$	3.774+1	3.82+1	3.990+1	3.613+1
	$^3\text{P}_1-^1\text{S}_0$	1.092+0	1.12+0	1.090+0	1.053+0		$^3\text{P}_1-^1\text{S}_0$	4.412+2	4.51+2	4.490+2	4.440+2
	$^3\text{P}_2-^1\text{S}_0$	2.129–3	2.35–3	2.278–3	2.148–3		$^3\text{P}_2-^1\text{S}_0$	2.853–1	3.00–1	2.839–1	2.786–1
	$^1\text{D}_2-^1\text{S}_0$	2.114+0	2.28+0	2.137+0	2.367+0		$^1\text{D}_2-^1\text{S}_0$	5.795+0	6.66+0	5.398+0	6.011+0
	$^3\text{P}_0-^3\text{P}_1$	1.266–3	1.28–3	1.233–3	1.270–3	16	$^3\text{P}_0-^3\text{P}_1$	2.520+0	2.54+0	2.519+0	2.519+0
	$^3\text{P}_0-^3\text{P}_2$	4.973–9	5.08–9	4.974–9	5.134–9		$^3\text{P}_0-^3\text{P}_2$	7.330–5	7.55–5	7.671–5	7.579–5
10	$^3\text{P}_1-^3\text{P}_2$	4.585–3	4.59–3	4.518–3	4.577–3		$^3\text{P}_1-^3\text{P}_2$	4.934+0	4.93+0	5.000+0	4.938+0
	$^3\text{P}_0-^1\text{D}_2$	1.936–5	2.37–5	3.063–5	2.503–5		$^3\text{P}_0-^1\text{D}_2$	1.768–3	2.02–3	2.525–3	2.190–3
	$^3\text{P}_1-^1\text{D}_2$	1.252–1	1.31–1	1.362–1	1.204–1		$^3\text{P}_1-^1\text{D}_2$	3.698+1	3.74+1	3.860+1	3.518+1
	$^3\text{P}_2-^1\text{D}_2$	3.499–1	3.65–1	3.818–1	3.365–1		$^3\text{P}_2-^1\text{D}_2$	7.578+1	7.66+1	7.999+1	7.216+1
	$^3\text{P}_1-^1\text{S}_0$	3.993+0	4.21+0	4.162+0	4.046+0		$^3\text{P}_1-^1\text{S}_0$	8.877+2	9.03+2	9.022+2	8.907+2
	$^3\text{P}_2-^1\text{S}_0$	6.289–3	6.69–3	6.532–3	6.226–3		$^3\text{P}_2-^1\text{S}_0$	5.186–1	5.42–1	5.130–1	5.021–1
	$^1\text{D}_2-^1\text{S}_0$	2.834+0	2.85+0	2.668+0	2.942+0		$^1\text{D}_2-^1\text{S}_0$	6.476+0	6.66+0	6.029+0	6.710+0
	$^3\text{P}_0-^3\text{P}_1$	6.111–3	6.06–3	5.966–3	6.123–3	17	$^3\text{P}_0-^3\text{P}_1$	6.709+0	6.56+0	6.727+0	6.707+0
	$^3\text{P}_0-^3\text{P}_2$	3.788–8	3.87–8	3.848–8	3.921–8		$^3\text{P}_0-^3\text{P}_2$	2.393–4	2.42–4	2.518–4	2.472–4
11	$^3\text{P}_1-^3\text{P}_2$	2.104–2	2.11–2	2.094–2	2.099–2		$^3\text{P}_1-^3\text{P}_2$	1.096+1	1.10+1	1.117+1	1.098+1
	$^3\text{P}_0-^1\text{D}_2$	5.007–5	5.97–5	7.580–5	6.330–5		$^3\text{P}_0-^1\text{D}_2$	3.135–3	3.59–3	4.548–3	3.929–3
	$^3\text{P}_1-^1\text{D}_2$	4.131–1	4.25–1	4.433–1	3.968–1		$^3\text{P}_1-^1\text{D}_2$	7.661+1	7.75+1	7.973+1	7.198+1
	$^3\text{P}_2-^1\text{D}_2$	1.119+0	1.15+0	1.206+0	1.075+0		$^3\text{P}_2-^1\text{D}_2$	1.449+2	1.47+2	1.528+2	1.370+2
	$^3\text{P}_1-^1\text{S}_0$	1.284+1	1.34+1	1.326+1	1.295+1		$^3\text{P}_1-^1\text{S}_0$	1.697+3	1.73+3	1.722+3	1.700+3
	$^3\text{P}_2-^1\text{S}_0$	1.589–2	1.68–2	1.635–2	1.572–2		$^3\text{P}_2-^1\text{S}_0$	9.132–1	9.55–1	8.911–1	8.730–1
	$^1\text{D}_2-^1\text{S}_0$	3.389+0	3.44+0	3.204+0	3.524+0		$^1\text{D}_2-^1\text{S}_0$	7.201+0	7.46+0	6.635+0	7.456+0

Table 5. continued

Z	Trans	Pres	NR	FS1	FS1c	Z	Trans	Pres	NR	FS1	FS1c
18	$^3P_0-^3P_1$	1.695+1	1.69+1	1.705+1	1.695+1	24	$^3P_0-^3P_1$	1.826+3	1.82+3	1.863+3	1.828+3
	$^3P_0-^3P_2$	7.241-4	7.38-4	7.675-4	7.478-4		$^3P_0-^3P_2$	1.679-1	1.73-1	1.946-1	1.730-1
	$^3P_1-^3P_2$	2.263+1	2.26+1	2.321+1	2.267+1		$^3P_1-^3P_2$	4.665+2	4.64+2	5.530+2	4.806+2
	$^3P_0-^1D_2$	5.380-3	6.13-3	8.033-3	6.889-3		$^3P_0-^1D_2$	7.261-2	8.47-2	1.974-1	1.553-1
	$^3P_1-^1D_2$	1.534+2	1.55+2	1.591+2	1.435+2		$^3P_1-^1D_2$	5.812+3	5.77+3	5.957+3	4.944+3
	$^3P_2-^1D_2$	2.660+2	2.68+2	2.806+2	2.493+2		$^3P_2-^1D_2$	6.038+3	5.97+3	6.475+3	5.292+3
	$^3P_1-^1S_0$	3.103+3	3.15+3	3.145+3	3.105+3		$^3P_1-^1S_0$	6.073+4	6.08+4	6.147+4	5.991+4
	$^3P_2-^1S_0$	1.567+0	1.63+0	1.503+0	1.473+0		$^3P_2-^1S_0$	2.717+1	2.73+1	2.233+1	2.207+1
	$^1D_2-^1S_0$	7.977+0	8.21+0	7.249+0	8.256+0		$^1D_2-^1S_0$	1.324+1	1.33+1	1.032+1	1.389+1
	$^3P_0-^3P_1$	4.088+1	3.96+1	4.122+1	4.088+1	25	$^3P_0-^3P_1$	3.509+3	3.48+3	3.590+3	3.514+3
19	$^3P_0-^3P_2$	2.051-3	1.99-3	2.192-3	2.117-3		$^3P_0-^3P_2$	3.555-1	3.62-1	4.228-1	3.659-1
	$^3P_1-^3P_2$	4.362+1	4.21+1	4.518+1	4.375+1		$^3P_1-^3P_2$	6.388+2	6.28+2	8.006+2	6.661+2
	$^3P_0-^1D_2$	8.991-3	1.02-2	1.397-2	1.186-2		$^3P_0-^1D_2$	9.848-2	1.61-1	3.338-1	2.586-1
	$^3P_1-^1D_2$	2.981+2	2.99+2	3.085+2	2.757+2		$^3P_1-^1D_2$	9.884+3	9.78+3	1.012+4	8.260+3
	$^3P_2-^1D_2$	4.718+2	4.77+2	4.985+2	4.377+2		$^3P_2-^1D_2$	9.690+3	9.54+3	1.041+4	8.442+3
	$^3P_1-^1S_0$	5.468+3	5.53+3	5.533+3	5.458+3		$^3P_1-^1S_0$	9.241+4	9.21+4	9.362+4	9.085+4
	$^3P_2-^1S_0$	2.627+0	2.72+0	2.473+0	2.425+0		$^3P_2-^1S_0$	4.175+1	4.15+1	3.320+1	3.300+1
	$^1D_2-^1S_0$	8.805+0	9.02+0	7.865+0	9.112+0		$^1D_2-^1S_0$	1.401+1	1.39+1	1.054+1	1.480+1
	$^3P_0-^3P_1$	9.440+1	9.44+1	9.558+1	9.440+1	26	$^3P_0-^3P_1$	6.540+3	6.53+3	6.708+3	6.554+3
	$^3P_0-^3P_2$	5.473-3	5.62-3	5.926-3	5.650-3		$^3P_0-^3P_2$	7.265-1	7.50-1	8.900-1	7.474-1
20	$^3P_1-^3P_2$	7.886+1	7.88+1	8.282+1	7.926+1		$^3P_1-^3P_2$	8.378+2	8.28+2	1.125+3	8.865+2
	$^3P_0-^1D_2$	1.458-2	1.68-2	2.404-2	2.013-2		$^3P_0-^1D_2$	1.277-1	1.51-1	5.679-1	4.338-1
	$^3P_1-^1D_2$	5.645+2	5.67+2	5.836+2	5.154+2		$^3P_1-^1D_2$	1.648+4	1.63+4	1.687+4	1.355+4
	$^3P_2-^1D_2$	8.138+2	8.17+2	8.629+2	7.470+2		$^3P_2-^1D_2$	1.543+4	1.50+4	1.660+4	1.341+4
	$^3P_1-^1S_0$	9.313+3	9.41+3	9.421+3	9.291+3		$^3P_1-^1S_0$	1.385+5	1.38+5	1.405+5	1.357+5
	$^3P_2-^1S_0$	4.320+0	4.43+0	3.971+0	3.902+0		$^3P_2-^1S_0$	6.356+1	6.26+1	4.885+1	4.895+1
	$^1D_2-^1S_0$	9.678+0	9.85+0	8.435+0	1.002+1		$^1D_2-^1S_0$	1.470+1	1.44+1	1.064+1	1.566+1
	$^3P_0-^3P_1$	2.093+2	2.10+2	2.121+2	2.094+2	27	$^3P_0-^3P_1$	1.183+4	1.19+4	1.217+4	1.187+4
	$^3P_0-^3P_2$	1.382-2	1.43-2	1.513-2	1.426-2		$^3P_0-^3P_2$	1.438+0	1.51+0	1.820+0	1.478+0
21	$^3P_1-^3P_2$	1.339+2	1.34+2	1.432+2	1.350+2		$^3P_1-^3P_2$	1.058+3	1.05+3	1.543+3	1.138+3
	$^3P_0-^1D_2$	2.293-2	2.65-2	4.095-2	3.381-2		$^3P_0-^1D_2$	1.579-1	1.88-1	9.746-1	7.346-1
	$^3P_1-^1D_2$	1.044+3	1.05+3	1.076+3	9.376+2		$^3P_1-^1D_2$	2.694+4	2.64+4	2.761+4	2.182+4
	$^3P_2-^1D_2$	1.374+3	1.38+3	1.459+3	1.244+3		$^3P_2-^1D_2$	2.436+4	2.35+4	2.625+4	2.122+4
	$^3P_1-^1S_0$	1.541+4	1.56+4	1.558+4	1.532+4		$^3P_1-^1S_0$	2.049+5	2.02+5	2.082+5	2.000+5
	$^3P_2-^1S_0$	6.989+0	7.13+0	6.278+0	6.161+0		$^3P_2-^1S_0$	9.606+1	9.32+1	7.129+1	7.220+1
	$^1D_2-^1S_0$	1.058+1	1.07+1	9.036+0	1.097+1		$^1D_2-^1S_0$	1.530+1	1.48+1	1.062+1	1.645+1
	$^3P_0-^3P_1$	4.466+2	4.48+2	4.535+2	4.467+2	28	$^3P_0-^3P_1$	2.084+4	2.11+4	2.149+4	2.092+4
	$^3P_0-^3P_2$	3.322-2	3.44-2	3.694-2	3.425-2		$^3P_0-^3P_2$	2.764+0	2.93+0	3.626+0	2.841+0
22	$^3P_1-^3P_2$	2.144+2	2.15+2	2.352+2	2.172+2		$^3P_1-^3P_2$	1.294+3	1.29+3	2.081+3	1.418+3
	$^3P_0-^1D_2$	3.493-2	4.05-2	6.935-2	5.635-2		$^3P_0-^1D_2$	1.851-1	2.16-1	1.690+0	1.258+0
	$^3P_1-^1D_2$	1.890+3	1.89+3	1.943+3	1.667+3		$^3P_1-^1D_2$	4.328+4	4.22+4	4.443+4	3.456+4
	$^3P_2-^1D_2$	2.279+3	2.27+3	2.429+3	2.039+3		$^3P_2-^1D_2$	3.816+4	3.63+4	4.112+4	3.341+4
	$^3P_1-^1S_0$	2.486+4	2.50+4	2.514+4	2.466+4		$^3P_1-^1S_0$	2.996+5	2.94+5	3.050+5	2.911+5
	$^3P_2-^1S_0$	1.113+1	1.13+1	9.730+0	9.560+0		$^3P_2-^1S_0$	1.443+2	1.38+2	1.033+2	1.060+2
	$^1D_2-^1S_0$	1.150+1	1.16+1	9.550+0	1.195+1		$^1D_2-^1S_0$	1.581+1	1.52+1	1.049+1	1.720+1
	$^3P_0-^3P_1$	9.188+2	9.20+2	9.352+2	9.194+2						
	$^3P_0-^3P_2$	7.628-2	7.89-2	8.643-2	7.860-2						
	$^3P_1-^3P_2$	3.246+2	3.25+2	3.684+2	3.313+2						
	$^3P_0-^1D_2$	5.134-2	5.97-2	1.170-1	9.353-2						
	$^3P_1-^1D_2$	3.349+3	3.34+3	3.437+3	2.901+3						
	$^3P_2-^1D_2$	3.731+3	3.70+3	3.988+3	3.298+3						
	$^3P_1-^1S_0$	3.924+4	3.94+4	3.969+4	3.882+4						
	$^3P_2-^1S_0$	1.750+1	1.77+1	1.484+1	1.461+1						
	$^1D_2-^1S_0$	1.239+1	1.25+1	9.984+0	1.293+1						

3.2. The oxygen isoelectronic sequence

The 12-configuration representation selected for the oxygen sequence is listed in Table 1. It may be seen that, in contrast to the calculation for the carbon sequence, the $P(4p)$ correlation orbital was found to be important. A comparison of the present theoretical energy separations with experiment, BZ and FS2 is given in Table 6. BZ used

the CI program CIV3 with BP relativistic corrections and their physical model includes extensive correlation within $n \leq 3$. FS2 used the MCHF+BP method with correlation configurations up to $n \leq 4$. It is found that the agreement between theory and experiment is very good (within 5%) except for the 1D_2 level in neutral oxygen ($Z = 8$). Generally speaking, BZ obtained the best accord with measurements.

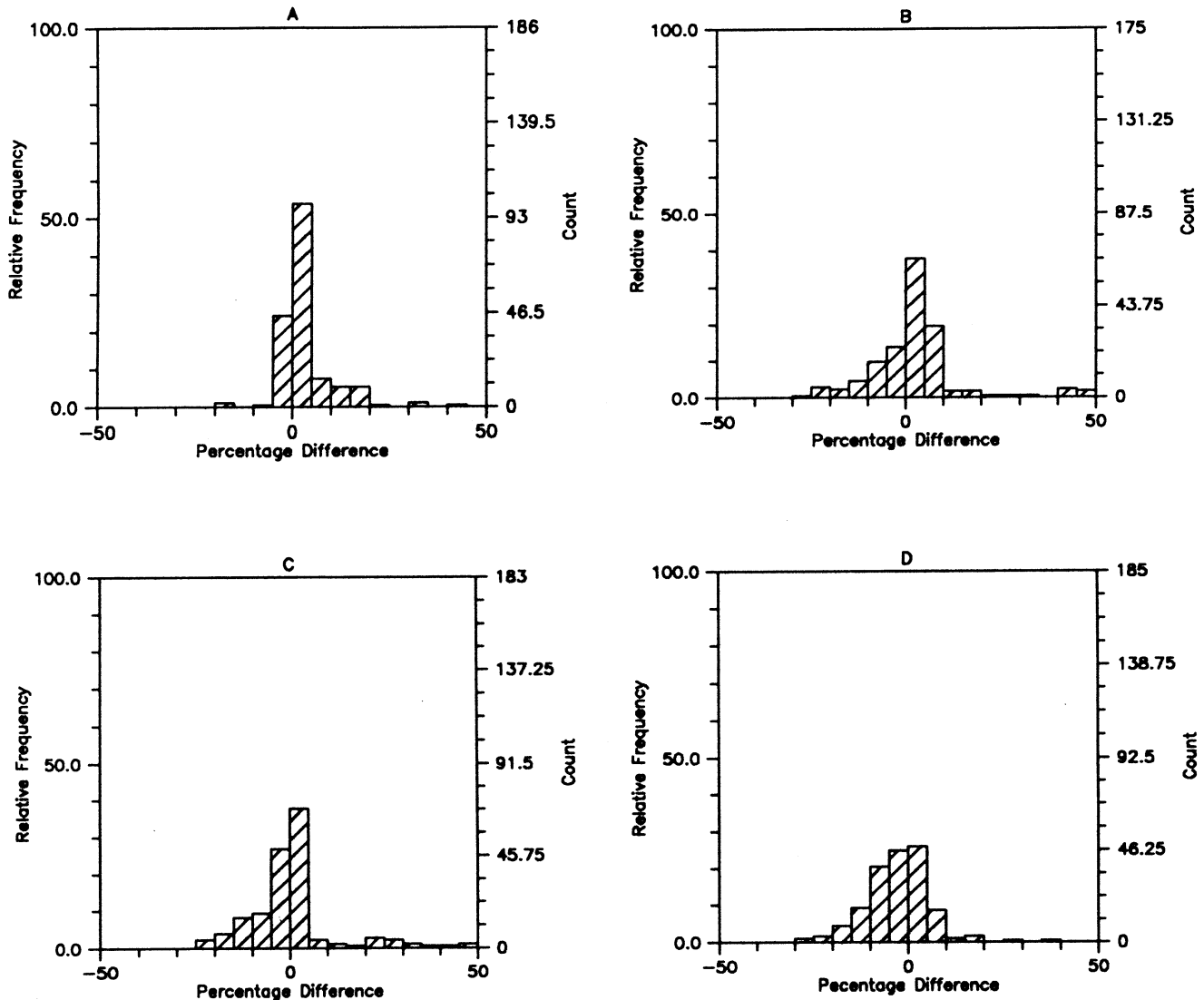


Fig. 1. Percentage difference histograms for the A -value data sets under consideration for the carbon sequence. **a)** NR and present excluding 1 A -value outside the 50% range; **b)** FS1 and present excluding 14 A -values; **c)** FS1c (wavelength corrected) and present excluding 7 A -values and **d)** FS1c (wavelength corrected) and NR excluding 6 A -values. It can be seen that the agreement with the FS1 data set is not greatly improved by the wavelength correction apart from reducing the number of A -values outside the 50% range

Present A -values for transitions within the ground configuration of this sequence are compared with BZ and FS2 in Table 7 and Fig. 2. Excellent agreement is found with BZ as 94% of the data agree to within 10% (see Fig. 2a). Differences larger than 10% are found at low Z ($Z \leq 12$) for the $^3P_0 - ^1D_2$ E2 transitions which, similar to the homologous case in the C sequence, have small line strengths and are sensitive to CI and the treatment of relativistic effects. The worst case is in O I where the discrepancy is as large as 41%. With regard to FS2, only 72% of the data agree with the present results to within 10% (see Fig. 2b), and large differences (up to a factor of 2) are noted for the difficult $^3P_0 - ^1D_2$ transitions. The very large

difference (a factor of 10) found for the $^3P_2 - ^3P_1$ transition for $Z = 13$ is believed to be due to a typographical error. In contrast with the C sequence, substantially improved accord is found if the FS2 A -values are corrected by substituting the experimental wavelengths (see FS2c in Table 7 and Fig. 2c): 83% of the data now agree to the desired accuracy (10%), and the discrepancies in the aforementioned E2 transition go down to the 30% level. The comparison between the BZ and FS2 datasets is interesting: although the 10% agreement level applies only to 71% of the data, this accuracy rating is reached by 93% of the A -values in FS2c (see Fig. 2d). Surprisingly, the larger differences ($\leq 23\%$) are not found in the $^3P_0 - ^1D_2$

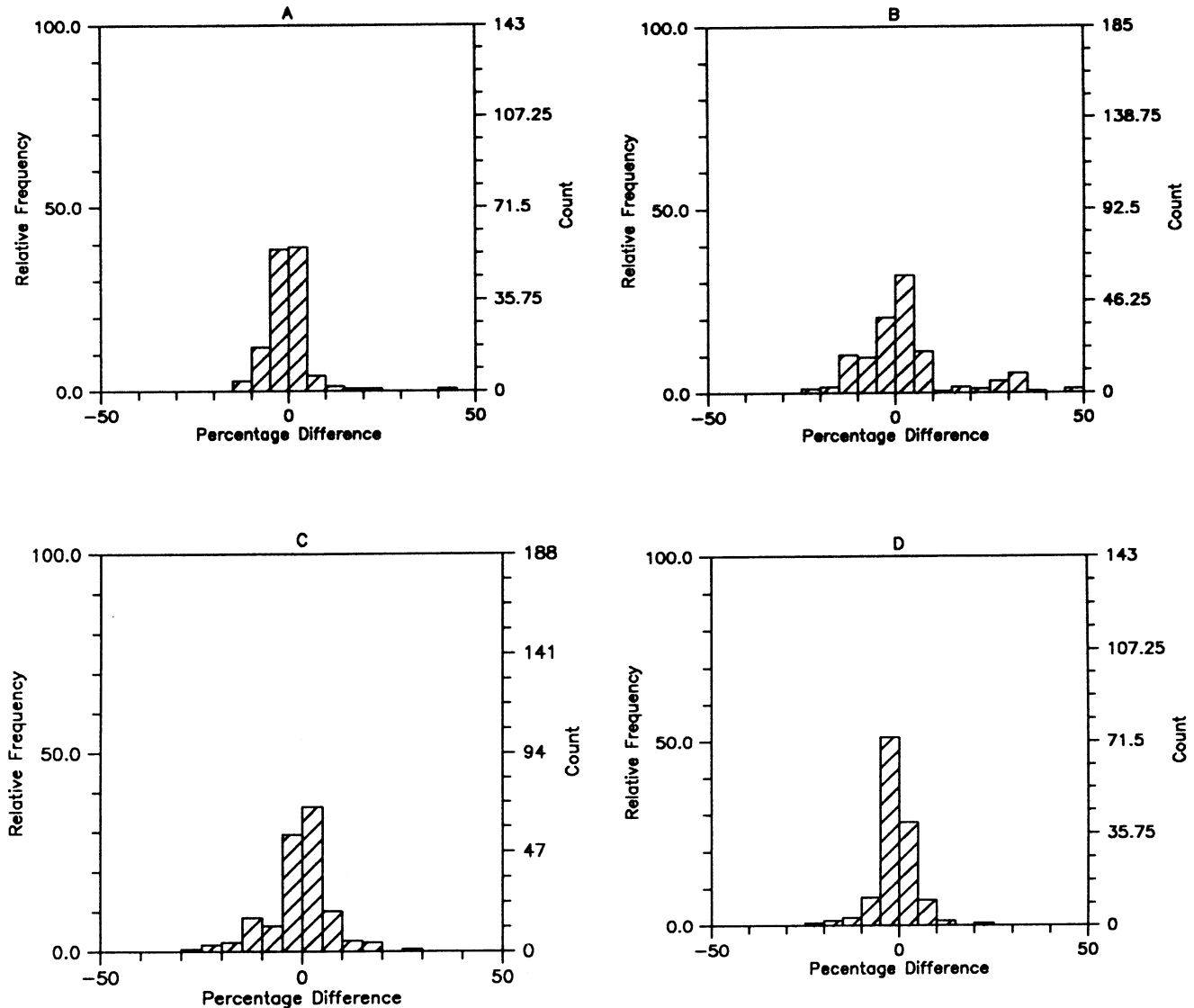


Fig. 2. Percentage difference histograms for the A -value data sets under consideration for the oxygen sequence. **a)** BZ and present; **b)** FS2 and present excluding 4 A -values outside the 50% range; **c)** FS2c (wavelength corrected) excluding 1 A -value; **d)** BZ and FS2c (wavelength corrected) excluding 1 A -value. The agreement with FS2 is significantly improved by the wavelength correction making its overall accuracy rating as reliable as the BZ and present datasets

transitions, as in the above comparisons with present results, but in other weak E2 transitions, i.e. ${}^3P_2 - {}^1S_0$ at low Z .

Note that BZ present a detailed comparison of their results with those of Cheng et al. (1979). The discussion will not be repeated here. The conclusion drawn by BZ is still valid: a “fully” relativistic calculation with little CI is reliable for high Z but not towards the neutral end of a given isoelectronic sequence.

In O I, the CD A -value calculated for transition ${}^1D_2 - {}^1S_0$ by Nicolaides et al. (1971) is close to the present result. Using many-body perturbation theory (MBPT), Gaigalas et al. (1994) obtained good agreement with the

line strengths of FS2 and BZ. Note that in their Tables X and XII the last two columns have been interchanged. The A -values recommended by BZ are in the column marked $A_{\text{s.e.}}^{\text{CI}}$.

For O I, Nicolaides et al. (1971) and BZ discuss some experimental results on the ratio $A(\lambda 5577)/A(\lambda 2972)$: 22 ± 2 (Le Blanc et al. 1966), 18.6 ± 3.7 (McConkey et al. 1966), on $A(\lambda 5577)$: 1.0 s^{-1} (McConkey & Kernahan 1969), on the lifetime of the 1S_0 state: $\leq 0.75 \text{ s}$ (Omholt 1956), 0.76 s (Corney & Williams 1972). The corresponding present values are respectively 14.2 , 1.124 , 0.83 , consistent with the experimental results. It should be noted that BZ can claim better overall

agreement. However, some of the experiments mentioned above are not accurate enough to draw definitive conclusions and there is a clear need for further measurements.

4. Conclusions

Several conclusions arise from this work. First, it has been shown that the reliability of A -values for the forbidden transitions within the ground configuration of the carbon and oxygen isoelectronic sequences depends strongly on the inclusion of a complete set of experimental level separations in the computations. Fortunately, in the present case, these are available from the excellent work of Edlén (1983, 1985). Therefore, the FS1 and FS2 datasets, which were calculated with theoretical level energy differences, must be corrected accordingly before they are used in astrophysical applications. For the oxygen sequence the independent BZ, FS2c and present datasets are of comparable accuracy. Most transition probabilities agree to within 10% except some small E2 A -values which are very sensitive to the numerical approximation even for large Z . In our opinion, it would be very difficult to improve their accuracy rating to better than the present 50%.

The standing discrepancies between FS1c and the present results for the carbon sequence are more difficult to explain. They are not reduced if the FS1 configuration expansion is reproduced or the TEC procedure is excluded in SUPERSTRUCTURE runs. The quality of the present radial wavefunctions for C-like ions appears to be established by the excellent agreement of the calculated excitation energies with experiment. Therefore, we are fairly confident about the reliability of the present computation for the carbon sequence. A 10% accuracy rating seems to be justified in this case, excluding of course the weak E2 transitions for $Z \leq 11$.

Acknowledgements. Part of the present work was carried out during visits by MEG and CM to the Observatoire de Paris, Meudon, France. The hospitality received is gratefully acknowledged. The visits were funded by IVIC, CONICIT, Fundación Polar, the Observatoire de Paris and the Ministère des Affaires Etrangères. This research has been supported by CONICIT under contract No. S1-95000521.

References

- Baluja K.L., Doyle J.G., 1981, J.Phys. B 14, L11
- Baluja K.L., Zeippen C.J., 1988, J.Phys. B 21, 1455 (BZ)
- Bhatia A.K., Feldman U., Doschek G.A., 1979, A&A 80, 22
- Biémont E., Hibbert A., Godefroid M., Vaeck N., 1993, ApJ 412, 431
- Biémont E., Zeippen C.J., 1991, J. Phys. IV C1, 209
- Biémont E., Zeippen C.J., 1996, Phys. Scri. T65, 192
- Cheng K.T., Kim Y.K., Desclaux J.P., 1979, At. Data Nucl. Data Tables 24, 111
- Corney A., Williams O.M., 1972, J. Phys. B 5, 686
- Edlén B., 1983, Phys. Scri. 28, 51
- Edlén B., 1985, Phys. Scri. 31, 345
- Eissner W., 1991, J. Phys. IV C1, 3
- Eissner W., Jones M., Nussbaumer H., 1974, Comput. Phys. Commun. 8, 270
- Eissner W., Nussbaumer H., 1969, J. Phys. B 2, 1028
- Froese Fischer C., Saha H.P., 1983, Phys. Rev. A 28, 3169 (FS2)
- Froese Fischer C., Saha H.P., 1985, Phys. Scri. 32, 181 (FS1)
- Gaigalas G., Kaniauskas, J., Kisielius R., Merkeliš, G., Vilkaš M.J., 1994, Phys. Scri. 49, 135
- Garstang R.H., 1968, Planetary Nebulae. In: Osterbrock D.E. & O'Dell C.R. (eds.). Reidel, Dordrecht p. 143
- Hibbert A., Biémont E., Godefroid M., Vaeck N., 1993, A&A 99, 179
- Hummer D.G., Berrington K.A., Eissner W., et al., 1993, A&A 279, 298 (IP)
- Jones M., 1970, J. Phys. B 3, 1571
- Jones M., 1971, J. Phys. B 4, 1422
- Kastner S.O., Bhatia A.K., Cohen L., 1977, Phys. Scri. 15, 259
- LeBlanc F.J., Oldenberg O., Carleton N.P., 1966, J.Chem. Phys. 45, 2200
- Mason H.E., Bhatia A.K., 1978, MNRAS 184, 423
- McConkey J.W., Burns D.J., Moran K.A., Emeleus K.G., 1966, Phys. Lett. 22, 416
- McConkey J.W., Kernahan J.A., 1969, Planetary Space Sci. 17, 1297
- Nicolaides C., Sinanoglu O., Westhaus P., 1971, Phys. Rev. A 4, 1400
- Nussbaumer H., 1971, ApJ 166, 411
- Nussbaumer H., Rusca C., 1979, A&A 72, 129 (NR)
- Nussbaumer H., Storey P.J., 1978, A&A 64, 139
- Omholz A., 1956, quoted by Nicolaides et al. (1971)
- Zeippen C.J., Seaton M.J., Morton D.C., 1977, MNRAS 181, 527

Table 6. Experimental and calculated excitation energies in cm^{-1} from the $2s^22p^4\ ^3P_2$ ground state for the oxygen sequence.
 Expt: experiment. Pres: present results. BZ: Baluja & Zeippen (1988). FS2: Froese Fischer & Saha (1983)

Z	State	Expt	Pres	BZ	FS2	Z	State	Expt	Pres	BZ	FS2
8	3P_1	158	158	155	157	19	3P_1	18945	18913	18874	18926
	3P_0	227	227	223	225		3P_0	23224	23032	22965	23019
	1D_2	15868	16787	16822	17067		1D_2	79589	81610	80686	81277
	1S_0	33793	34813	34125	34256		1S_0	162868	163181	162541	161965
9	3P_1	341	338	335	338	20	3P_1	24465	24467	24411	24541
	3P_0	490	485	480	485		3P_0	28880	28651	28569	28892
	1D_2	20873	21974	21798	22137		1D_2	88202	90300	89371	90607
	1S_0	44918	45719	45015	45419		1S_0	178568	178786	178220	179705
10	3P_1	643	633	631	637	21	3P_1	31183	31241		31320
	3P_0	921	908	903	911		3P_0	35259	34980		35309
	1D_2	25841	27290	26735	27124		1D_2	97846	100043		100391
	1S_0	55751	56710	55723	56254		1S_0	195975	196097		197142
11	3P_1	1107	1092	1088	1097	22	3P_1	39277	39425	39294	39503
	3P_0	1576	1556	1549	1562		3P_0	42309	41956	41840	42404
	1D_2	30841	32396	31710	32134		1D_2	108717	111038	110082	111435
	1S_0	66496	67425	66397	66284		1S_0	215509	215544	215121	216724
12	3P_1	1783	1763	1758	1771	23	3P_1	48939	49211		49290
	3P_0	2521	2494	2483	2501		3P_0	49944	49474		50086
	1D_2	35925	37553	36798	37233		1D_2	121025	123502		123956
	1S_0	77287	78167	77140	77730		1S_0	237651	237626		238941
13	3P_1	2733	2706	2700	2717	24	3P_1	60375	60834	60563	60896
	3P_0	3827	3787	3774	3798		3P_0	58050	57416	57287	58239
	1D_2	41147	42827	42028	42477		1D_2	134991	137675	136649	138186
	1S_0	88206	88988	88015	88581		1S_0	262926	262908	262523	264336
14	3P_1	4028	3992	3985	4007	25	3P_1	73800	74513	74013	74548
	3P_0	5568	5510	5494	5526		3P_0	66505	65618	65456	66731
	1D_2	46568	48289	47465	47927		1D_2	150851	153806	152596	154374
	1S_0	99343	100014	99118	99626		1S_0	291899	291907	291339	293493
15	3P_1	5748	5701		5723	26	3P_1	89439	90495	89889	90486
	3P_0	7817	7738		7759		3P_0	75188	73950	73888	75428
	1D_2	52256	54026		53653		1D_2	168848	172149	170885	172776
	1S_0	110799	111402		110960		1S_0	325149	325326	324893	327017
16	3P_1	7985	7931	7923	7957	27	3P_1	107527	109032		108962
	3P_0	10648	10545	10519	10569		3P_0	83992	82276		84213
	1D_2	58295	60117	59247	59741		1D_2	189233	192978		193660
	1S_0	122700	123245	122428	122699		1S_0	363262	363760		365521
17	3P_1	10847	10791		10819	28	3P_1	128308	130396	129337	130237
	3P_0	14127	13997		14019		3P_0	92836	90484	90688	92989
	1D_2	64782	66667		66291		1D_2	212262	216573	214958	217304
	1S_0	135206	135706		134986		1S_0	406819	407805	407163	409616
18	3P_1	14455	14406	14384	14429						
	3P_0	18307	18149	18101	18160						
	1D_2	71834	73784	72875	73423						
	1S_0	148513	148908	148205	148000						

Table 7. Transition probabilities in s^{-1} within the ground state configuration of the oxygen sequence. Pres: present results. BZ: Baluja & Zeippen (1988). FS2: Froese Fischer & Saha (1983). FS2c: FS2 corrected with the experimental wavelengths. $a \pm b$ denotes $a \times 10^{\pm b}$

Z	Trans	Pres	BZ	FS2	FS2c	Z	Trans	Pres	BZ	FS2	FS2c
8	${}^3P_2 - {}^3P_1$	8.865–5	8.957–5	8.702–5	8.869–5	14	${}^3P_2 - {}^3P_1$	1.465+0	1.472+0	1.447+0	1.470+0
	${}^3P_2 - {}^3P_0$	1.275–10	1.203–10	1.409–10	1.473–10		${}^3P_2 - {}^3P_0$	2.072–5	2.070–5	2.072–5	2.152–5
	${}^3P_1 - {}^3P_0$	1.772–5	1.735–5	1.705–5	1.781–5		${}^3P_1 - {}^3P_0$	1.964–1	1.973–1	1.885–1	1.964–1
	${}^3P_2 - {}^1D_2$	6.535–3	5.627–3	7.056–3	5.694–3		${}^3P_2 - {}^1D_2$	1.232+1	1.183+1	1.278+1	1.173+1
	${}^3P_1 - {}^1D_2$	2.111–3	1.818–3	2.283–3	1.834–3		${}^3P_1 - {}^1D_2$	3.139+0	3.016+0	3.285+0	2.986+0
	${}^3P_0 - {}^1D_2$	6.388–7	8.992–7	1.197–6	8.269–7		${}^3P_0 - {}^1D_2$	2.110–4	2.270–4	2.689–4	2.273–4
	${}^3P_2 - {}^1S_0$	2.945–4	2.732–4	2.250–4	2.102–4		${}^3P_2 - {}^1S_0$	1.032–1	9.810–2	9.132–2	9.003–2
	${}^3P_1 - {}^1S_0$	7.909–2	7.601–2	7.789–2	7.475–2		${}^3P_1 - {}^1S_0$	1.397+2	1.414+2	1.409+2	1.396+2
	${}^1D_2 - {}^1S_0$	1.124+0	1.215+0	1.057+0	1.304+0		${}^1D_2 - {}^1S_0$	5.721+0	5.792+0	5.317+0	5.894+0
	${}^3P_2 - {}^3P_1$	8.912–4	8.910–4	8.680–4	8.913–4	15	${}^3P_2 - {}^3P_1$	4.248+0		4.211+0	4.266+0
9	${}^3P_2 - {}^3P_0$	1.985–9	1.980–9	2.110–9	2.221–9		${}^3P_2 - {}^3P_0$	7.736–5		7.689–5	7.981–5
	${}^3P_1 - {}^3P_0$	1.784–4	1.803–4	1.702–4	1.772–4		${}^3P_1 - {}^3P_0$	4.754–1		4.533–1	4.757–1
	${}^3P_2 - {}^1D_2$	3.941–2	3.546–2	4.203–2	3.532–2		${}^3P_2 - {}^1D_2$	2.794+1		2.888+1	2.670+1
	${}^3P_1 - {}^1D_2$	1.249–2	1.124–2	1.337–2	1.118–2		${}^3P_1 - {}^1D_2$	6.597+0		6.893+0	6.299+0
	${}^3P_0 - {}^1D_2$	2.618–6	3.252–6	4.204–6	3.108–6		${}^3P_0 - {}^1D_2$	3.832–4		4.828–4	4.110–4
	${}^3P_2 - {}^1S_0$	1.257–3	1.162–3	1.029–3	9.735–4		${}^3P_2 - {}^1S_0$	1.876–1		1.658–1	1.646–1
	${}^3P_1 - {}^1S_0$	4.690–1	4.650–1	4.693–1	4.537–1		${}^3P_1 - {}^1S_0$	3.135+2		3.154+2	3.137+2
	${}^1D_2 - {}^1S_0$	1.828+0	1.939+0	1.724+0	2.026+0		${}^1D_2 - {}^1S_0$	6.588+0		6.073+0	6.757+0
10	${}^3P_2 - {}^3P_1$	5.974–3	6.005–3	5.809–3	5.975–3	16	${}^3P_2 - {}^3P_1$	1.136+1	1.141+1	1.130+1	1.142+1
	${}^3P_2 - {}^3P_0$	2.081–8	2.103–8	2.164–8	2.285–8		${}^3P_2 - {}^3P_0$	2.574–4	2.559–4	2.545–4	2.642–4
	${}^3P_1 - {}^3P_0$	1.159–3	1.163–3	1.112–3	1.161–3		${}^3P_1 - {}^3P_0$	1.010+0	1.015+0	9.529–1	1.010+0
	${}^3P_2 - {}^1D_2$	1.730–1	1.602–1	1.834–1	1.588–1		${}^3P_2 - {}^1D_2$	5.952+1	5.745+1	6.137+1	5.705+1
	${}^3P_1 - {}^1D_2$	5.344–2	4.951–2	5.689–2	4.902–2		${}^3P_1 - {}^1D_2$	1.284+1	1.240+1	1.341+1	1.230+1
	${}^3P_0 - {}^1D_2$	8.269–6	9.759–6	1.217–5	9.450–6		${}^3P_0 - {}^1D_2$	6.585–4	6.929–4	8.246–4	7.044–4
	${}^3P_2 - {}^1S_0$	3.985–3	3.762–3	3.415–3	3.265–3		${}^3P_2 - {}^1S_0$	3.218–1	3.054–1	2.829–1	2.829–1
	${}^3P_1 - {}^1S_0$	2.028+0	2.049+0	2.056+0	2.000+0		${}^3P_1 - {}^1S_0$	6.592+2	6.655+2	6.616+2	6.611+2
	${}^1D_2 - {}^1S_0$	2.563+0	2.677+0	2.422+0	2.764+0		${}^1D_2 - {}^1S_0$	7.514+0	7.536+0	6.856+0	7.681+0
	${}^3P_2 - {}^3P_1$	3.048–2	3.064–2	2.972–2	3.054–2	17	${}^3P_2 - {}^3P_1$	2.837+1		2.834+1	2.856+1
11	${}^3P_2 - {}^3P_0$	1.599–7	1.616–7	1.644–7	1.719–7		${}^3P_2 - {}^3P_0$	7.739–4		7.612–4	7.910–4
	${}^3P_1 - {}^3P_0$	5.562–3	5.586–3	5.409–3	5.550–3		${}^3P_1 - {}^3P_0$	1.879+0		1.745+0	1.879+0
	${}^3P_2 - {}^1D_2$	6.149–1	5.788–1	6.472–1	5.729–1		${}^3P_2 - {}^1D_2$	1.204+2		1.239+2	1.157+2
	${}^3P_1 - {}^1D_2$	1.837–1	1.729–1	1.943–1	1.709–1		${}^3P_1 - {}^1D_2$	2.340+1		2.447+1	2.249+1
	${}^3P_0 - {}^1D_2$	2.202–5	2.510–5	3.055–5	2.455–5		${}^3P_0 - {}^1D_2$	1.081–3		1.353–3	1.156–3
	${}^3P_2 - {}^1S_0$	1.066–2	1.014–2	9.310–3	9.460–3		${}^3P_2 - {}^1S_0$	5.247–1		4.577–1	4.614–1
	${}^3P_1 - {}^1S_0$	7.152+0	7.249+0	7.253+0	7.321+0		${}^3P_1 - {}^1S_0$	1.313+3		1.314+3	1.320+3
	${}^1D_2 - {}^1S_0$	3.315+0	3.427+0	3.132+0	3.886+0		${}^1D_2 - {}^1S_0$	8.532+0		7.685+0	8.702+0
	${}^3P_2 - {}^3P_1$	1.273–1	1.279–1	1.249–1	1.275–1	18	${}^3P_2 - {}^3P_1$	6.682+1	6.716+1	6.700+1	6.736+1
	${}^3P_2 - {}^3P_0$	9.683–7	9.737–7	9.863–7	1.026–6		${}^3P_2 - {}^3P_0$	2.125–3	2.107–3	2.079–3	2.165–3
12	${}^3P_1 - {}^3P_0$	2.166–2	2.178–2	2.102–2	2.172–2		${}^3P_1 - {}^3P_0$	3.024+0	3.037+0	2.745+0	3.021+0
	${}^3P_2 - {}^1D_2$	1.868+0	1.775+0	1.954+0	1.757+0		${}^3P_2 - {}^1D_2$	2.329+2	2.258+2	2.394+2	2.243+2
	${}^3P_1 - {}^1D_2$	5.348–1	5.080–1	5.629–1	5.026–1		${}^3P_1 - {}^1D_2$	4.019+1	3.895+1	4.202+1	3.868+1
	${}^3P_0 - {}^1D_2$	5.146–5	5.724–5	6.862–5	5.647–5		${}^3P_0 - {}^1D_2$	1.712–3	1.774–3	2.151–3	1.834–3
	${}^3P_2 - {}^1S_0$	2.499–2	2.378–2	2.204–2	2.142–2		${}^3P_2 - {}^1S_0$	8.196–1	7.764–1	7.057–1	7.180–1
	${}^3P_1 - {}^1S_0$	2.157+1	2.186+1	2.184+1	2.145+1		${}^3P_1 - {}^1S_0$	2.497+3	2.515+3	2.491+3	2.518+3
	${}^1D_2 - {}^1S_0$	4.090+0	4.191+0	3.852+0	4.281+0		${}^1D_2 - {}^1S_0$	9.692+0	9.705+0	8.589+0	9.870+0
	${}^3P_2 - {}^3P_1$	4.580–1	4.603–1	4.513+0	4.593+0	19	${}^3P_2 - {}^3P_1$	1.497+2	1.503+2	1.505+2	1.510+2
	${}^3P_2 - {}^3P_0$	4.849–6	4.854–6	4.890–6	5.080–6		${}^3P_2 - {}^3P_0$	5.364–3	5.321–3	5.221–3	5.458–3
13	${}^3P_1 - {}^3P_0$	7.051–2	7.076–2	6.806–2	7.055–2		${}^3P_1 - {}^3P_0$	4.107+0	4.125+0	3.592+0	4.104+0
	${}^3P_2 - {}^1D_2$	5.030+0	4.812+0	5.236+0	4.763+0		${}^3P_2 - {}^1D_2$	4.142+2	4.219+2	4.462+2	4.191+2
	${}^3P_1 - {}^1D_2$	1.366+0	1.307+0	1.433+0	1.293+0		${}^3P_1 - {}^1D_2$	6.237+1	6.355+1	6.857+1	6.311+1
	${}^3P_0 - {}^1D_2$	1.085–4	1.185–4	1.409–4	1.178–4		${}^3P_0 - {}^1D_2$	2.757–3	2.720–3	3.353–3	2.843–3
	${}^3P_2 - {}^1S_0$	5.292–2	5.037–2	4.685–2	4.587–2		${}^3P_2 - {}^1S_0$	1.092+0	1.165+0	1.041+0	1.070+0
	${}^3P_1 - {}^1S_0$	5.761+1	5.835+1	5.820+1	5.741+1		${}^3P_1 - {}^1S_0$	4.562+3	4.589+3	4.535+3	4.620+3
	${}^1D_2 - {}^1S_0$	4.891+0	4.979+0	4.579+0	5.073+0		${}^1D_2 - {}^1S_0$	1.107+1	1.106+1	9.613+0	1.126+1

Table 7. continued

Z	Trans	Pres	BZ	FS2	FS2c	Z	Trans	Pres	BZ	FS2	FS2c
20	$^3P_2 - ^3P_1$	3.195+2	3.213+2	3.198+2	3.168+2	25	$^3P_2 - ^3P_1$	8.264+3	8.330+3	8.409+3	8.159+3
	$^3P_2 - ^3P_0$	1.256-2	1.244-2	1.277-2	1.274-2		$^3P_2 - ^3P_0$	3.152-1	3.101-1	3.229-1	3.175-1
	$^3P_1 - ^3P_0$	4.453+0	4.475+0	4.263+0	4.454+0		$^3P_1 - ^3P_0$	5.819+0	5.858+0	7.184+0	5.839+0
	$^3P_2 - ^1D_2$	7.858+2	7.640+2	8.087+2	7.463+2		$^3P_2 - ^1D_2$	1.082+4	1.053+4	1.110+4	1.036+4
	$^3P_1 - ^1D_2$	1.018+2	9.890+1	1.074+2	9.648+1		$^3P_1 - ^1D_2$	5.256+2	5.096+2	5.569+2	5.008+2
	$^3P_0 - ^1D_2$	4.028-3	4.121-3	5.430-3	4.456-3		$^3P_0 - ^1D_2$	4.039-2	4.021-2	5.269-2	4.350-2
	$^3P_2 - ^1S_0$	1.786+0	1.687+0	1.587+0	1.537+0		$^3P_2 - ^1S_0$	7.694+0	7.155+0	6.541+0	6.365+0
	$^3P_1 - ^1S_0$	8.052+3	8.095+3	8.098+3	7.933+3		$^3P_1 - ^1S_0$	9.312+4	9.265+4	9.265+4	9.158+4
	$^1D_2 - ^1S_0$	1.277+1	1.276+1	1.213+1	1.302+1		$^1D_2 - ^1S_0$	3.639+1	3.617+1	3.464+1	3.711+1
	$^3P_2 - ^3P_1$	6.557+2		6.581+2	6.495+2		$^3P_2 - ^3P_1$	1.449+4	1.461+4	1.480+4	1.429+4
21	$^3P_2 - ^3P_0$	2.731-2		2.787-2	2.767-2	26	$^3P_2 - ^3P_0$	4.999-1	4.907-1	5.109-1	5.028-1
	$^3P_1 - ^3P_0$	3.444+0		3.230+0	3.446+0		$^3P_1 - ^3P_0$	4.150+1	4.182+1	4.917+1	4.168+1
	$^3P_2 - ^1D_2$	1.383+3		1.422+3	1.317+3		$^3P_2 - ^1D_2$	1.738+4	1.692+4	1.783+4	1.665+4
	$^3P_1 - ^1D_2$	1.516+2		1.601+2	1.439+2		$^3P_1 - ^1D_2$	6.689+2	6.484+2	7.089+2	6.370+2
	$^3P_0 - ^1D_2$	6.122-3		8.169-3	6.719-3		$^3P_0 - ^1D_2$	7.074-2	7.002-2	9.222-2	7.603-2
	$^3P_2 - ^1S_0$	2.513+0		2.225+0	2.160+0		$^3P_2 - ^1S_0$	9.712+0	9.052+0	8.110+0	7.881+0
	$^3P_1 - ^1S_0$	1.379+4		1.384+4	1.358+4		$^3P_1 - ^1S_0$	1.431+5	1.421+5	1.421+5	1.406+5
	$^1D_2 - ^1S_0$	1.497+1		1.422+1	1.526+1		$^1D_2 - ^1S_0$	4.902+1	4.868+1	4.681+1	5.002+1
	$^3P_2 - ^3P_1$	1.296+3	1.304+3	1.305+3	1.283+3	27	$^3P_2 - ^3P_1$	2.478+4		2.542+4	2.443+4
	$^3P_2 - ^3P_0$	5.545-2	5.477-2	5.671-2	5.608-2		$^3P_2 - ^3P_0$	7.528-1		7.662-1	7.562-1
22	$^3P_1 - ^3P_0$	1.387+0	1.392+0	1.215+0	1.387+0		$^3P_1 - ^3P_0$	1.781+2		2.083+2	1.791+2
	$^3P_2 - ^1D_2$	2.380+3	2.318+3	2.444+3	2.270+3		$^3P_2 - ^1D_2$	2.752+4		2.825+4	2.637+4
	$^3P_1 - ^1D_2$	2.171+2	2.111+2	2.296+2	2.066+2		$^3P_1 - ^1D_2$	8.328+2		8.827+2	7.924+2
	$^3P_0 - ^1D_2$	9.404-3	9.521-3	1.244-2	1.025-2		$^3P_0 - ^1D_2$	1.282-1		1.674-1	1.376-1
	$^3P_2 - ^1S_0$	3.440+0	3.231+0	3.027+0	2.943+0		$^3P_2 - ^1S_0$	1.212+1		9.892+0	9.590+0
	$^3P_1 - ^1S_0$	2.298+4	2.304+4	2.302+4	2.264+4		$^3P_1 - ^1S_0$	2.166+5		2.147+5	2.126+5
	$^1D_2 - ^1S_0$	1.793+1	1.786+1	1.702+1	1.827+1		$^1D_2 - ^1S_0$	6.804+1		6.525+1	6.947+1
	$^3P_2 - ^3P_1$	2.478+3		2.503+3	2.450+3	28	$^3P_2 - ^3P_1$	4.142+4	4.185+4	4.267+4	4.080+4
	$^3P_2 - ^3P_0$	1.053-1		1.079-1	1.064-1		$^3P_2 - ^3P_0$	1.082+0	1.058+0	1.095+0	1.086+0
	$^3P_1 - ^3P_0$	4.910-2		2.446-2	4.923-2		$^3P_1 - ^3P_0$	5.796+2	5.863+2	6.760+2	5.838+2
	$^3P_2 - ^1D_2$	4.011+3		4.117+3	3.833+3		$^3P_2 - ^1D_2$	4.302+4	4.182+4	4.418+4	4.119+4
	$^3P_1 - ^1D_2$	3.004+2		3.179+2	2.861+2		$^3P_1 - ^1D_2$	1.017+3	9.833+2	1.078+3	9.665+2
	$^3P_0 - ^1D_2$	1.478-2		1.942-2	1.602-2		$^3P_0 - ^1D_2$	2.386-1	2.339-1	3.130-1	2.561-1
	$^3P_2 - ^1S_0$	4.587+0		4.007+0	3.900+0		$^3P_2 - ^1S_0$	1.499+1	1.412+1	1.190+1	1.150+1
	$^3P_1 - ^1S_0$	3.741+4		3.738+4	3.683+4		$^3P_1 - ^1S_0$	3.236+5	3.195+5	3.202+5	3.172+5
	$^1D_2 - ^1S_0$	2.203+1		2.092+1	2.246+1		$^1D_2 - ^1S_0$	9.695+1	9.628+1	9.348+1	9.907+1
	$^3P_2 - ^3P_1$	4.591+3	4.624+3	4.654+3	4.536+3						
24	$^3P_2 - ^3P_0$	1.878-1	1.850-1	1.925-1	1.894-1						
	$^3P_1 - ^3P_0$	1.959-1	1.971-1	2.930-1	1.963-1						
	$^3P_2 - ^1D_2$	6.643+3	6.473+3	6.815+3	6.355+3						
	$^3P_1 - ^1D_2$	4.029+2	3.916+2	4.267+2	3.839+2						
	$^3P_0 - ^1D_2$	2.397-2	2.402-2	3.136-2	2.589-2						
	$^3P_2 - ^1S_0$	5.993+0	5.594+0	5.176+0	5.039+0						
	$^3P_1 - ^1S_0$	5.959+4	5.953+4	5.942+4	5.864+4						
	$^1D_2 - ^1S_0$	2.787+1	2.771+1	2.649+1	2.842+1						